INFLUENCES INVESTIGATION OF NUMERICAL PARAMETERS AND MESHING ON THE AEROELASTIC RESPONSE

T. F. G. Costa, E. M. Belo
School of Engineering of Sao Carlos – University of Sao Paulo, Brazil

Keywords: *flutter, aeroelasticity, non-stationary aerodynamics, vortex-lattice method*

Abstract

The purpose of this work is to simulate several aeroelastic responses of an aircraft wing in the time domain in order to compare the influence of some numerical parameters. The main objective is to provide knowledge of using these parameters to increase accuracy with the minimum increase of computational effort on numerical flutter simulations. For the simulations proposed, a numerical model of a finite flexible wing is firstly developed and implemented computationally.

The aeroelastic response is obtained in time domain as a result of the numeric integration of the motion equations of the structure. These equations represent the wing structural dynamics excited by aerodynamics non-stationary loads. The structure is modeled by Finite Element Method (using NASTRAN®), and the aerodynamics is modeled using non-stationary vortex-lattice method (using FORTRAN90 language). The coupling of both models meshes is done using a surface spline method.

The main parameters analyzed deal with the mesh and integration step.

Conclusions indicate the best ways to improve aeroelastic model accuracy.

1 Introduction

Aeroelastic phenomena are characterized by the coupling of elastic, inertia and aerodynamic forces [11] [12]. Basically it relates structural flexibility with non-stationary aerodynamic flow [11].

With constant aircraft optimization, structures tend to be lighter, commonly leading to more flexibility, where flutter analysis becomes essential [11].

The flutter can be studied in frequency domain [13], where flutter critical speed can be determined with some accuracy, and in the time domain, where the aeroelastic response in time can be found [14].

Flutter numerical simulations demand a huge computational effort. This problem becomes more serious in time domain simulations.

The proposed method to reduce computational effort is to determine which numerical parameters are critical, and what are their influences over simulation time. This work will provide information for future studies to balance in a convenient way the computational effort and the accuracy of results.

The parameters analyzed are: mesh refinement spanwise and chordwise, wake length, wake model, integration step, and wing airfoil.

The greatest accuracy can be achieved using the most refined mesh, with the maximum wake length, and minimum time interval, but, this model would be extremely slow to simulate. This work compiles lots of information useful to preview time spent on future aeroelastic simulations.

2 The Numerical Model

2.1 The Wing Simulated

A real wing with experimental modal analysis data available [3] was taken as reference for this entire work. The wing is rectangular with a 2.980m span and 0.220m chord, with no sweep

and no dihedral. Its structure is composed by a Styrofoam core, unidirectional carbon fiber span and a bi-directional kevlar shell [2]. The airfoil is a Selig S1223 [2] [10]. A material properties table and details of the finite element model used to represent wing structure can be found in reference [4].

The mathematical model to represent this wing is composed by:

- A finite element structural mesh for modal analysis, adjusted to obtain the same natural frequencies as the experiment [3] [4];
- A vortex-lattice mesh for non-stationary aerodynamic analysis.

2.2 Finite Element Structural Model

The matrix equation used to describe the harmonic oscillatory motion, not excited and not damped, of a flexible linear structure [1] is given by:

$$[M]\{\ddot{x}(t)\}+[K]\{x(t)\}=0 \qquad (1)$$

where: $[M]$ = Mass matrix;

$[K]$ = Elastic matrix;

$\{x(t)\}$ = Displacements vector, as function of time.

In case of a structure excited by forces $\{F\}$ dependant on structure geometry, structure displacement velocity and time, equation (1) can be rewritten as:

$$[M]\{\ddot{x}(t)\}+[K]\{x(t)\}=\{F(t,x(t),\dot{x}(t))\} \qquad (2)$$

However, finite element models usually have a large number of degrees of freedom, what leads to a high order of $[M]$ and $[K]$.

To simplify the model order the structure harmonic motion can be described as a linear composition of the natural modes. It is known that only the low frequencies are relevant. So, equation (2) becomes:

$$\{\ddot{\eta}(t)\}+\left[\omega^2\right]\{\eta(t)\}=\left[\hat{\Phi}\right]^T\{F(t,x(t),\dot{x}(t))\} \qquad (3)$$

where: $\left[\omega^2\right]$ = Matrix with the natural frequencies in the diagonal;

$\{\eta(t)\}$ = Modal displacement vector, as function of time.

$\left[\hat{\Phi}\right]^T$ = Matrix with one natural mode per row, which is the transposed of the classic eigenvalue solution $[\Phi]$, normalized with respect to the inertia matrix according to:

$$\left[\hat{\Phi}\right]=[\Phi][M]^{-1/2} \qquad (4)$$

The transformation between $\{x(t)\}$ and $\{\eta(t)\}$ is:

$$\{x(t)\}=\left[\hat{\Phi}\right]\{\eta(t)\} \qquad (5)$$

$$\{\ddot{x}(t)\}=\left[\hat{\Phi}\right]\{\ddot{\eta}(t)\} \qquad (6)$$

2.3 Vortex-Lattice Aerodynamic Model

The vortex-lattice method consists in divide the wing platform in several panels. Each panel has a closed vortex ring, respecting Helmholtz theorem [5].

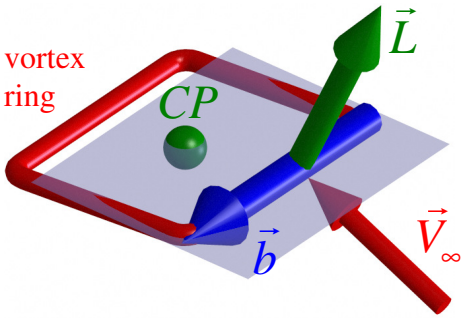

Fig. 1 – The vortex-lattice panels, vortex ring and reference vectors.

where: $\vec{V}_\infty$ = Free flow velocity;

$\vec{b}$ = Panel span;

$\vec{L}$ = Lift;

CP = Control point.

The lift of the wing is a composition of the lift of all panels. The equation used to calculate panel lift is obtained from Bernoulli equation [5] and prepared to be used in an iterative process [4] [6] as:

$$L=\left[\rho\Gamma(t)\left(\vec{V}_\infty\times\vec{b}\right)+S_{pn}\rho\frac{\Gamma(t)-\Gamma(t-\Delta t)}{\Delta t}\vec{N}_{pn}\right]\cdot\vec{N}_w \qquad (7)$$

where: L = Lift as a scalar number;

$\Gamma(t)$ = Vortex ring intensity (vorticity), as function of time;

S_{pn} = Panel area;

$\vec{N}_{pn}$ = Unitary vector normal to panel plane;

$\vec{N}_{w}$ = Unitary vector normal to wing plane.

In order to solve the aerodynamic model, and find the components of all aerodynamic forces perpendicular to the wing, it is necessary to determine the vorticity distribution over the wing.

In each control point of the aerodynamic model, the velocity induced by all vortex ring can be found imposing that the velocity component perpendicular to the wing should be zero to guarantee that there is no airflow crossing wing surface. The following equation is obtained:

$$\sum_{j=1}^{n_{wing}} \vec{N}_i \cdot \vec{V}_{ij}\,\Gamma_j = -\vec{N}_i \cdot \left(\vec{V}_\infty + \vec{V}_{pc_i} + \sum_{k=1}^{n_{wake}} V_{ik} \right) \qquad (8)$$

where: $\vec{N}_i$ = Unitary vector normal to panel i;

Γ_i = Vortex ring intensity of panel i;

$\vec{V}_{pc_i}$ = Control point velocity due to flexible motion of the structure;

V_{ij} = Induced velocity of o wing panel j on the control point of panel i;

V_{ik} = Induced velocity of a wake panel k on the control point of panel i;

n_{wing} = Number of panels in wing mesh;

n_{wake} = Number of panels in wake mesh;

Using equation (8) for all wing panels, a linear system is obtained. Its solution is the vorticity distribution.

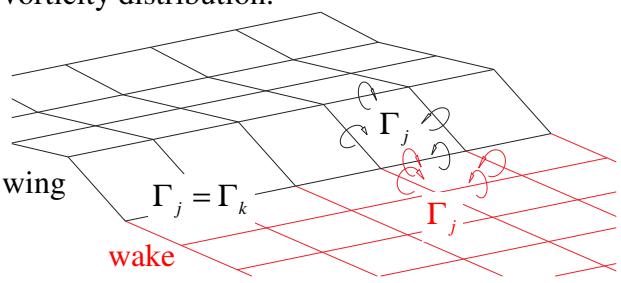

Fig. 2 – Kutta condition

Kutta condition states that the intensity of the vortex at the trailing edge should be zero [7]. To satisfy Kutta condition each first panel of the wake must have the same intensity of the wing panel in front of it (Fig. 2)..

The induced velocities V_{ij} and V_{ik} are calculated according to the Biot-Savart law [7] [5] (Fig. 3 and equation (9)).

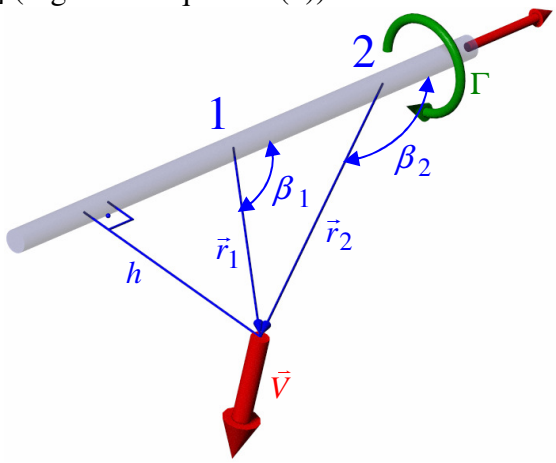

Fig. 3 – Biot-Savrat law, simplified to a straight vortex segment [5].

$$\vec{V} = \frac{\Gamma}{4\pi} \frac{\vec{r}_1 \times \vec{r}_2}{\left|\vec{r}_1 \times \vec{r}_2\right|^2} \left(\frac{\vec{r}}{|\vec{r}|} - \frac{\vec{r}_2}{|\vec{r}_2|} \right) \cdot \left(\vec{r}_1 - \vec{r}_2 \right) \qquad (9)$$

The induced velocities V_{ij} and V_{ik} for the entire ring are just the sum of the induced velocities of each segment of the ring calculated with equation (9).

2.4 Surface Spline Method for Coupling Meshes

The coupling of aerodynamic and structural models is important, since the forces obtained in the aerodynamic mesh (equation (7)) should be used in equation (3), that is written in structural mesh. At the same time, the motion obtained on the solution of equation (3) should be transported to aerodynamic mesh to solve the load distribution (equations (7), (8) and (9)).

The surface spline interpolation method [8] is very useful in this case. Interpolating the structural mesh to find the same mode shapes in aerodynamic mesh for control points and for vortex ring vertices, it is possible to do the following conversions [4] [6]:

$$\{\bar{z}_a\} = [G]\{\bar{z}_s\} \quad (10)$$

$$\{\dot{\bar{z}}_a\} = [G]\{\dot{\bar{z}}_s\} \quad (11)$$

$$\{F_s\} = [G]^T \{F_a\} \quad (12)$$

where: $\{\bar{z}\}$ = Vector of nodal displacements normal to the wing plane;

$\{\dot{\bar{z}}\}$ = Vector of nodal velocities normal to the wing plane;

$\{F\}$ = Vector of forces normal do the wing plane;

s = subscript relative to structural mesh;

a = subscript relative to aerodynamic mesh;

$[G]$ = transformation matrix. The procedure to determine this matrix in found in references [4] [6] and [8];

Since the modal matrix is a matrix composed of several vectors of structural displacements, equation (3) can be rewritten as:

$$\{\ddot{\eta}(t)\} + [\omega^2]\{\eta(t)\} = \left[\hat{\Phi}_a\right]^T \{F_a(t, x(t), \dot{x}(t))\} \quad (13)$$

where: $\left\{\hat{\Phi}_a\right\}^T$ = transposed of the modal matrix written in coordinates of the control points of the aerodynamic mesh.

2.5 Integration Method

Finally, equation (13) can describe the physics of the aeroelastic model, relating aerodynamic forces and inertia forces. However, it can't be solved analytically, since the vector $\{F_a\}$, containing the forces, can't be described as a mathematical equation. It is result of all the procedure described in section 2.3.

A numerical integration is used to solve equation (13). The predictor-corrector method was used in form PECLE, described by Lambert [9], using the collection of methods Adams-Bashforth for predictor step and Adams-Moulton for corrector step [9] [4] [6]. This method is used solve first order differential equations. Therefore equation (13) should reduced to:

$$\begin{aligned} \dot{X}_1 &= X_2 \\ \dot{X}_2 &= \left[\hat{\Phi}_a\right]^T \{F_a(t, x(t), \dot{x}(t))\} - [\omega^2] X_1 \end{aligned} \quad (14)$$

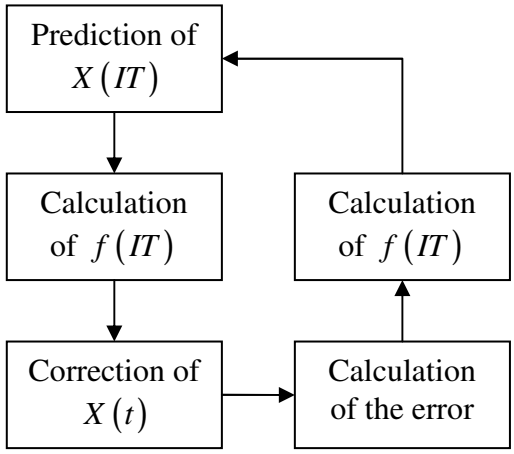

Fig. 4 – Predictor-corrector in form PECLE

where: IT = Iteration number;

X = Left hand side of system equation (14);

f = Right hand side of system equation (14).

3 Simulations and Results

The main objective of this work was to qualify, for the methods described in section 2, which are the most significant parameters to accuracy and computational effort.

The results were organized in different sections, from 3.1 to 3.6. These parameters were not studied together to avoid mistaken conclusions.

Results concerning time spent in computational simulation should be considered comparatively, since the absolute value is applicable only to a machine with the same specification of the computer where calculations were performed (AMD Athlon™ XP 2400+ 2.00GHz, 512 Mb RAM).

3.1 Integration step

According to the simulations performed with different steps of time in the integration process, one can note (Fig. 5 and Fig. 6) that this parameter affects mostly the frequency of the harmonic motion.

The error in frequency can be noted by the difference in phase at instant 0.3s (Fig. 5 and Fig. 6).

If accuracy in frequency is not so important for the case studied, time step may be increased reducing computational effort. This effect is presented in Fig. 7.

For these simulations, the following parameters were used:

- flat plate airfoil
- air density: 1.225kg/m^3
- wing angle of attack: 5º
- speed: 100m/s
- wake truncation length: 1.0m
- simulation total time: 0.300s
- number of panels chordwise: 8
- number of panels spanwise: 13
- wake model: flat

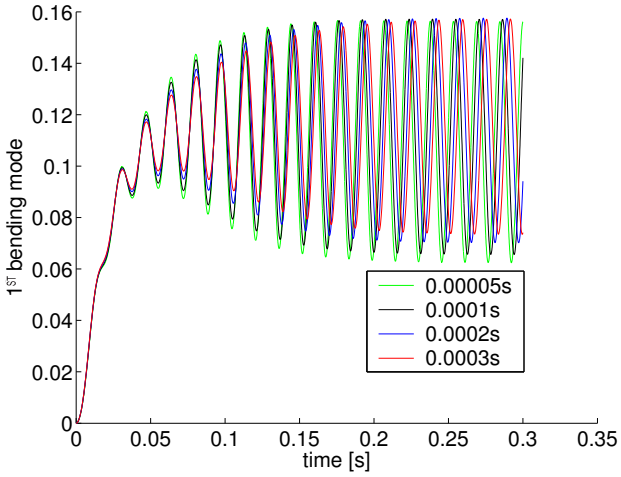

Fig. 5 – Behavior of 1st bending mode for different integration steps.

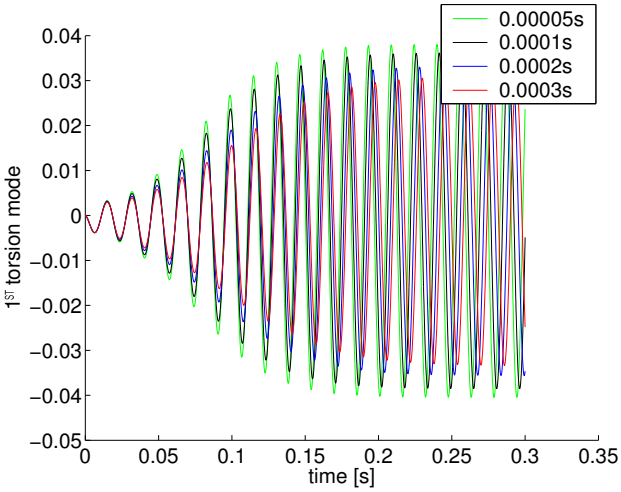

Fig. 6 – Behavior of 1st torsion mode for different integration steps.

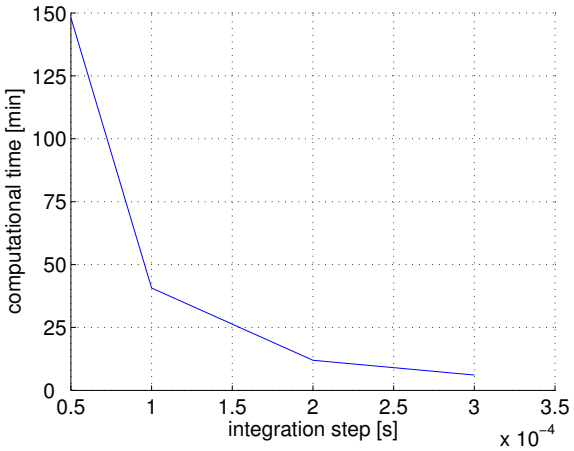

Fig. 7 – Variation of computational time according to the integration step.

3.2 Spanwise Refinement

Several simulations were performed to compare the aeroelastic response in time for different spanwise refinements keeping 4 panels chordwise.

The results can be seen in Fig. 8 and Fig. 9. One can note that all results are very close. A small difference is shown in the equilibrium value.

The main conclusion is that the spanwise refinement has a small effect on the displacement of the deformed wing. However, increased mesh refinement comes at a considerably computational effortas may be seen from Fig. 10.

For these simulations, the following parameters were used:

- flat plate airfoil
- air density: 1.225kg/m^3
- wing angle of attack: 5º
- speed: 100m/s
- wake truncation length: 1.0m
- simulation total time: 0.300s
- number of panels chordwise: 4
- integration step: 0.0001s
- wake model: flat

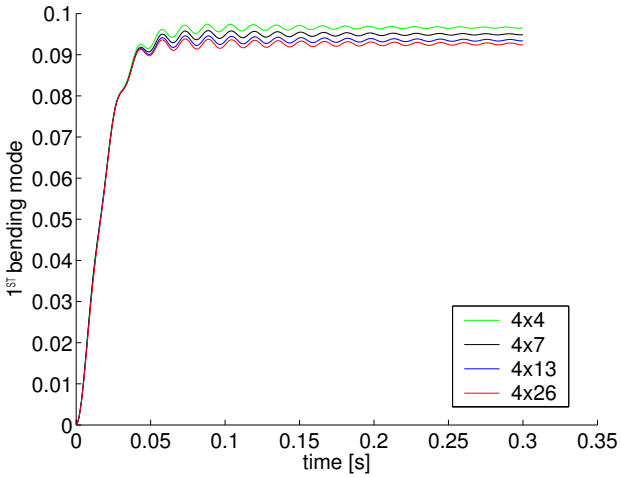

Fig. 8 – Behavior of 1st bending mode for an aerodynamic mesh with 4 panels chordwise and different cases of spanwise refinement.

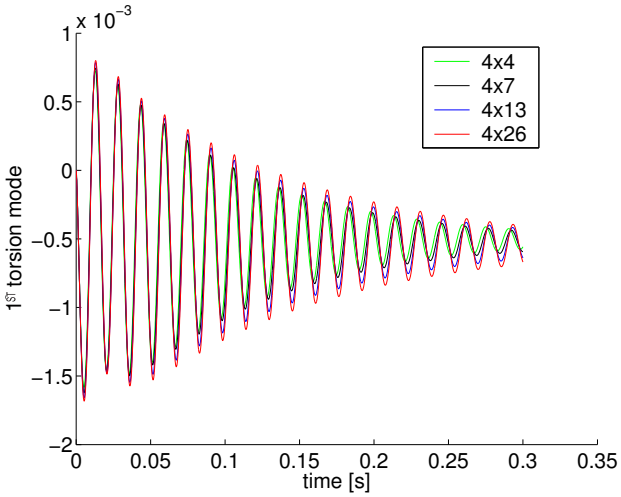

Fig. 9 – Behavior of 1st torsion mode for an aerodynamic mesh with 4 panels chordwise and different cases of spanwise refinement.

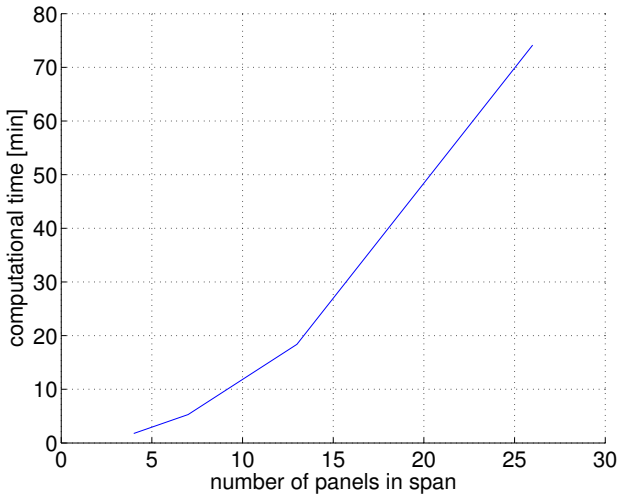

Fig. 10 – Variation of computational time according to the mesh spanwise refinement.

3.3 Chordwise Refinement

Several simulations were performed to compare the aeroelastic response in time for different chordwise refinements keeping 13 panels spanwise.

The results can be seen in Fig. 11 and Fig. 12. One can note that for 8 and 10 panels chordwise, the response behavior is very close.

As the number of panels chordwise increases, the accuracy of load distribution chordwise gets better. This affects directly the excitation of the torsion modes and consequently, the *flutter* phenomenon.

Fig. 13 shows the time spent in these simulations. The behavior of computational effort is almost linear.

The obvious conclusion is the importance of the chordwise refinement, since the linear variation of computational effort is not critical and the gain in accuracy with the refinement is very significant.

For these simulations the following parameters were used:

- flat plate airfoil
- air density: 1.225kg/m^3
- wing angle of attack: 5º
- speed: 100m/s
- wake truncation length: 1.0m
- simulation total time: 0.300s
- number of panels spanwise: 13
- integration step: 0.0001s
- wake model: flat

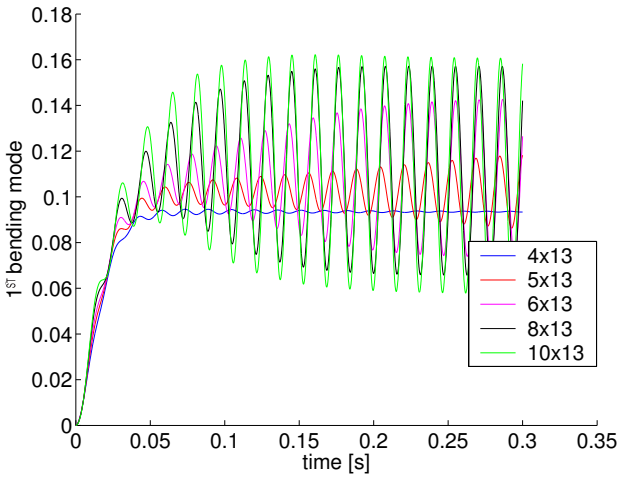

Fig. 11 – Behavior of 1st bending mode for an aerodynamic mesh with 13 panels spanwise and different cases of chordwise refinement.

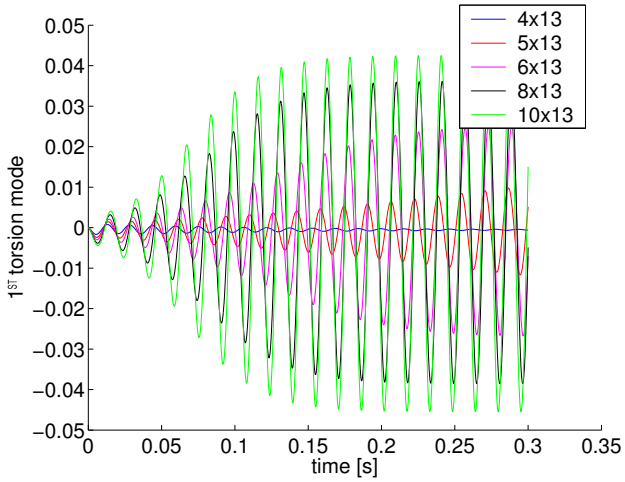

Fig. 12 – Behavior of 1st torsion mode for an aerodynamic mesh with 13 panels spanwise and different cases of chordwise refinement.

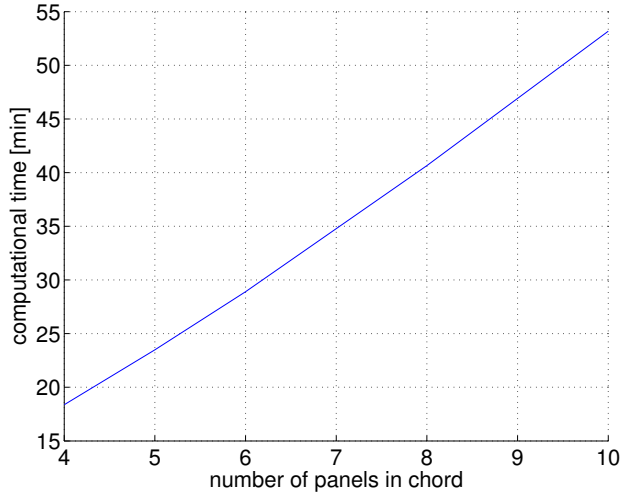

Fig. 13 – Variation of computational time according to the mesh chordwise refinement.

3.4 Wake Length

The wake is created along the simulation, and the first point created gets farther from the wing at each iteration. Considering that distant wake points does not affect the wing load, a truncation process was used to reduce the number of elements in the wake mesh.

The complete wake, without any truncation, was used as reference to calculate the error in aeroelastic response for truncated cases. The parameter used to calculate the error is the value of the exponential behavior of the aeroelastic response.

For a wake of only 4.0m (134.23% of span) the results are very close to the complete wake (22.5 m)

Fig. 14 to Fig. 17 show the results obtained. Clearly, the wake truncation is a good option to enhance accuracy and reduction of computational effort. The model with a 4.0m truncated wake reaches solution in 4.56 hours, while the complete wake model spent 13.61 hours with almost no gain in accuracy.

For these simulations were used:

- flat plate airfoil
- air density: 1.225kg/m^3
- wing angle of attack: 5º
- speed: 75m/s
- simulation total time: 0.300s
- number of panels chordwise: 8
- number of panels spanwise: 13
- integration step: 0.00008s
- wake model: flat

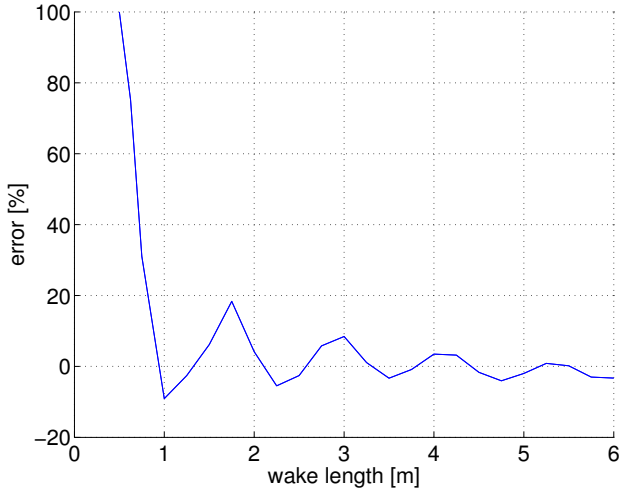

Fig. 14 – Error on intensity of exponential behavior of the damped harmonic motion for the 1st bending mode, according to the wake length

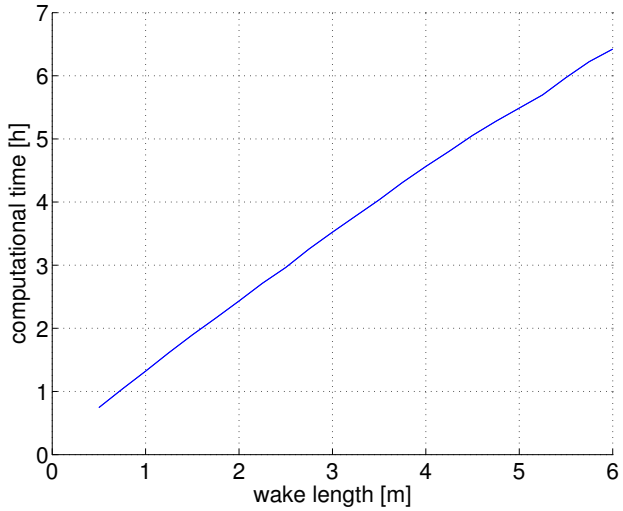

Fig. 15 – Variation of computational time according to wake length

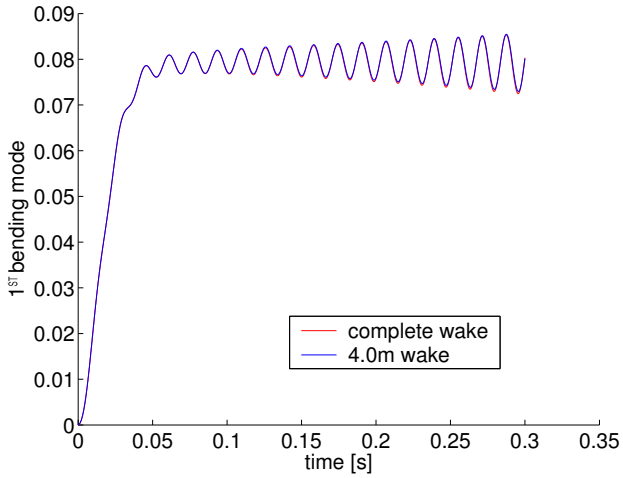

Fig. 16 – Behavior of 1st bending mode for cases with complete wake (no truncation) and 4.0 meters wake.

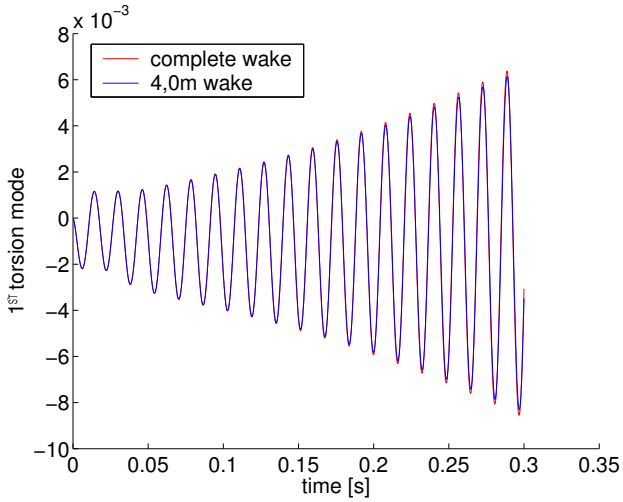

Fig. 17 – Behavior of 1st torsion mode for cases with complete wake (no truncation) and 4.0 meters wake.

3.5 Wake Model

Two types of wake models were studied. The first one was called *"flat" wake*. In this model the motion of the wake is determined only by the free flow speed. So, in a stationary simulation the wake geometry is flat. In non-stationary simulation the geometry of the wake is a history of the trailing edge positions along time.

The second model is called *free wake*. In this model the wake position is influenced by the velocity induced by all vortex rings of the model. This results in much more computational effort and has no advantage in terms of accuracy. The flat wake model reaches the solution in just 3.56 hours, while free wake model spent 89.06 hours with no significant changes in solution. The results can be seen in Fig. 18 and Fig. 19.

For these simulations, the following parameters were used:

- flat plate airfoil
- air density: 1.225kg/m^3
- wing angle of attack: 5º
- speed: 75m/s
- wake truncation length: 4.0m
- simulation total time: 0.150s
- number of panels chordwise: 8
- number of panels spanwise: 13
- integration step: 0.00008s

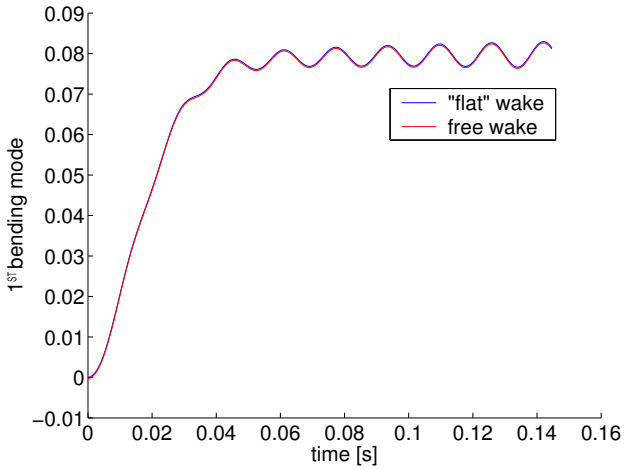

Fig. 18 – Behavior of 1st bending mode for cases with flat wake and free wake.

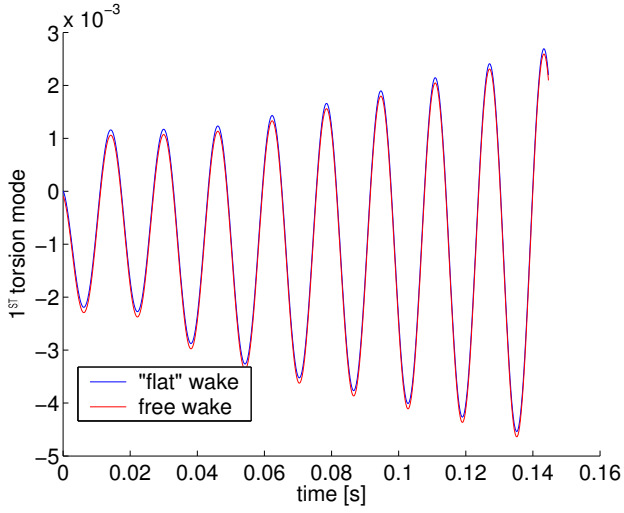

Fig. 19 – Behavior of 1st torsion mode for cases with flat wake and free wake.

3.6 Use of Camber Line

To study the influence of a more precise airfoil model, two cases were analyzed. The first one is a flat plate airfoil and the second is a camber line that results, at 5º angle of attack, the same lift and moment coefficients as the real wing airfoil (Selig S1223).

Both cases were simulated below and above flutter critical speed (which is about 70m/s).

One can note, from Fig. 21 to Fig. 24, that the most important difference between both cases is that they oscillate around different positions for the same angle of attack. Adjusting the angle of attack of the flat plate to obtain the same lift as the cambered airfoil (Fig. 21), the torsion is still far from the correct response (Fig. 22). It is not possible, using a flat plate, to get precise response for bending and moment at the same time. At high speeds (Fig. 23 and Fig. 24), bending is more coupled to torsion, which makes impossible a good adjustment for lift as in low speed case.

The use of a camber line appears to be unnecessary to determination of flutter critical speed, but it is important to accuracy of the motion amplitude. The motion amplitude in bending and torsion affects several structural parameters requiring accuracy, therefore the use of a camber line shows to be a good option, with no increase of computational effort.

For these simulations were used:

- air density: 1.225kg/m^3
- wing angle of attack: 5º
- speed: 75m/s
- wake truncation length: 4.0m
- simulation total time: 0.300s
- number of panels chordwise: 8
- number of panels spanwise: 13
- integration step: 0.00008s
- wake model: flat

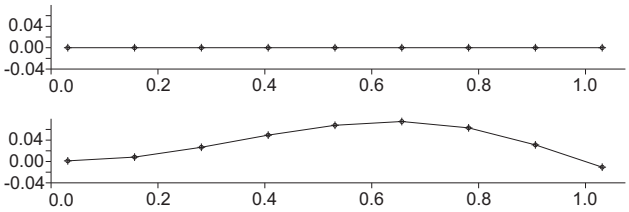

Fig. 20 – Flat plate and camber line airfoils. This camber line results in C_L = 1.5094 and C_M = -0.290 at 5º angle of attack (same as Selig S1223)

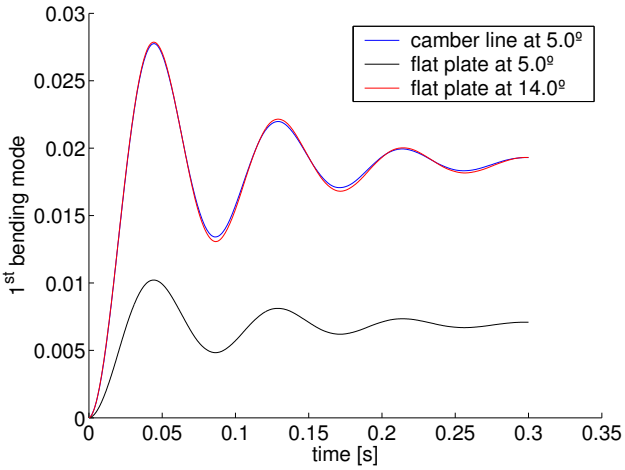

Fig. 21 – Behavior of 1st bending mode at 20.0m/s for cases with flat plate and camber line airfoils.

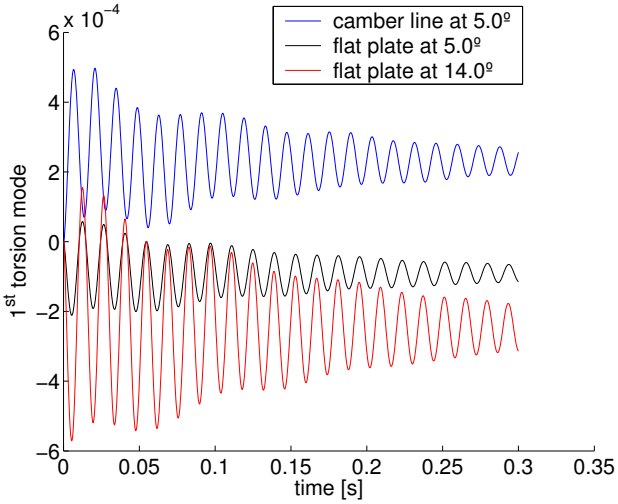

Fig. 22 – Behavior of 1st torsion mode at 20.0m/s for cases with flat plate and camber line airfoils.

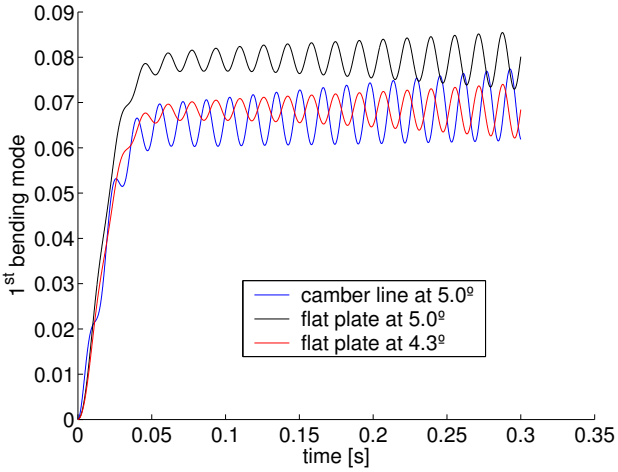

Fig. 23 – Behavior of 1st bending mode at 75.0m/s for cases with flat plate and camber line airfoils.

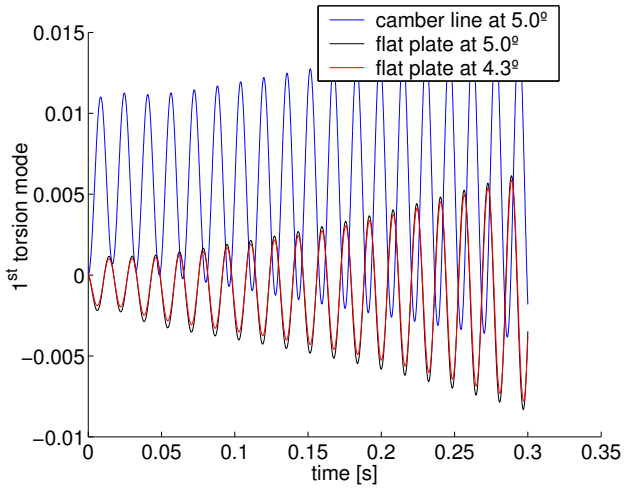

Fig. 24 – Behavior of 1st torsion mode at 75.0m/s for cases with flat plate and camber line airfoils.

4 Conclusions

This work presented a compilation of several time domain aeroelastic numeric simulations of a wing, relating numerical parameters to solution accuracy and computational effort.

The main conclusions are:

- Integration time step: affects the frequency of the solution harmonic motion. The data presented can help find the balance between accuracy for the response frequency and computational effort.

- Spanwise refinement: does not show a significant advantage due to large increases in computational time for small improvements in aeroelastic response.

- Chordwise refinement: is the most critical of the variables chosen. It affects significantly the behavior of the aeroelastic response. If a poor refinement is used, there is a risk of substantial error in the convergence/divergence characteristic of the response.

- Wake length: the process of truncating the wake length leads to a significant gain in computational effort with no significant losses in accuracy.

- Camber line airfoil: is a good option, since it does not increase computational effort and allow a better understanding of the aeroelastic response.

References

[1] Craig Jr., R. R. *Structural Dynamics: an Introduction to Computer Methods.* John Wiley & Sons, Inc, 1981.

[2] Equipe EESC-USP de AeroDesign (2002). *Technical Report – AeroDesign East 2002*. Titusville, 2002.

[3] Marques, F. D.; Varoto, P. S.; Benini, G. R.; Oliveira, L. P. R. An investigation on the modal characteristics of an aircraft wing structure. In: Espíndola, J. J. et al. ads., *Dynamic Problems of Mechanics.* Rio de Janeiro. ABCM. pp. 465-469, 2001.

[4] Costa, T. F. G. *Numeric study of a wing with flutter active control by feedback of the pressure measured in one point.* 122pp. Dissertation (M. Sc.) – Engineering School of Sao Carlos, University of Sao Paulo, Sao Carlos, 2007.

[5] Katz, J.; Plotkin, A. *Low-Speed Aerodynamics.* 2ªed Cambridge University Press, 2001.

[6] Benini, G. R. *Modelo Numérico para Simulação da Resposta Aeroelástica de Asas Fixas. Dissertação (Mestrado)* – Escola de Engenharia de São Carlos, Universidade de São Paulo, 2001.

[7] Anderson, J. D. *Fundamentals of aerodynamics*. 2ªed McGraw-Hill, Inc, 1991

[8] Harder, R. L.; Desmarais, R. N. *Interpolation Using Surface Splines*. Journal of Aircraft; Vol. 9, nº 2, p.189-191, 1972

[9] Lambert, J. D. *Numerical Methods for Ordinary Differential Systems: The Initial Value Problem.* John Wiley & Sons, Inc, 1991

[10] Selig M. UIUC Low-Speed Airfoil Tests. http://www.ae.uiuc.edu/mselig/pub/LSATs/AppendedFiles_vol1/LIFT01.TXT (30 march, 2006)

[11] Bisplinghoff, R. L.; Ashley, H.; Halfman, R. L. *Aeroelasticity*. Dover Publications, Inc., Mineola – NY, 1996.

[12] Collar, A R. *The Expanding Domain of Aeroelasticity*. The Journal of the Royal Aeronautical Society; Vol 50, p.613-636, 1946.

[13] Theodorsen, T. General Theory of Aerodynamic Instability and the Mechanism of Flutter. *NACA Technical Report 496*, 1935.

[14] Strganac, T. W.; Mook, D. T. Numerical Model of Unsteady Subsonic Aeroelastic Behavior. *AIAA Journal*; Vol. 28, nº 5, p.903-909, 1990.

Copyright Statement

The authors confirm that they, and/or their company or institution, hold copyright on all of the original material included in their paper. They also confirm they have obtained permission, from the copyright holder of any third party material included in their paper, to publish it as part of their paper. The authors grant full permission for the publication and distribution of their paper as part of the ICAS2008 proceedings or as individual off-prints from the proceedings.